
Data Quality in Imitation Learning

Suneel Belkhale
Stanford University
belkhale@stanford.edu

Yuchen Cui
Stanford University
yuchenc@stanford.edu

Dorsa Sadigh
Stanford University
dorsa@stanford.edu

Abstract

In supervised learning, the question of data quality and curation has been overshadowed in recent years by increasingly more powerful and expressive models that can ingest internet-scale data. However, in offline learning for robotics, we simply lack internet scale data, and so high quality datasets are a necessity. This is especially true in imitation learning (IL), a sample efficient paradigm for robot learning using expert demonstrations. Policies learned through IL suffer from state distribution shift at test time due to compounding errors in action prediction, which leads to unseen states that the policy cannot recover from. Instead of designing new algorithms to address distribution shift, an alternative perspective is to develop new ways of assessing and curating datasets. There is growing evidence that the same IL algorithms can have substantially different performance across different datasets. This calls for a formalism for defining metrics of “data quality” that can further be leveraged for data curation. In this work, we take the first step toward formalizing data quality for imitation learning through the lens of distribution shift: a high quality dataset encourages the policy to stay in distribution at test time. We propose two fundamental properties that shape the quality of a dataset: i) *action divergence*: the mismatch between the expert and learned policy at certain states; and ii) *transition diversity*: the noise present in the system for a given state and action. We investigate the combined effect of these two key properties in imitation learning theoretically, and we empirically analyze models trained on a variety of different data sources. We show that state diversity is not always beneficial, and we demonstrate how action divergence and transition diversity interact in practice.

1 Introduction

Supervised learning methods have seen large strides in recent years in computer vision (CV), natural language processing (NLP), and human-level game playing [18, 26, 42, 8, 49, 13, 43]. These domains have benefited from large and complex models that are trained on massive internet-scale datasets. Despite their undeniable power, biases present in these large datasets can result in the models exhibiting unexpected or undesirable outcomes. For example, foundation models such as GPT-3 trained on uncensored datasets have resulted in instances of racist behavior such as associating Muslims with violence [1, 5]. Thus offline data curation is immensely important for both safety and cost-effectiveness, and it is gaining in prominence in training foundation models [22, 10, 39].

Data curation is even more important in the field of robotics, where internet-scale data is not readily available and real-world datasets are small and uncensored. Noise or biases present in the data can lead to dangerous situations in many robotics tasks, for example injuring a person or damaging equipment. In such scenarios, deciding which data to collect and how best to collect it are especially important [36, 33, 4]. Of course, the quality of data depends on the algorithm that uses the data. A common paradigm in robot learning from offline datasets is imitation learning (IL), a data-driven, sample efficient framework for learning robot policies by mimicking expert demonstrations. However, when learning from offline data using IL, estimating data quality becomes especially difficult, since the “test set” the robot is evaluated on is an entirely new data distribution due to compounding errors

incurred by the model, i.e., action prediction errors take the model to unseen states. This phenomenon is studied and referred to as the distribution shift problem, and prior work has viewed and addressed it through several angles [45, 48].

Broadly, prior work address distribution shift either by taking an *algorithm-centric* approach to account for biases in the dataset, or by directly modifying the dataset collection process in a *data-centric* manner. Algorithm-centric approaches learn robust policies by imposing task-specific assumptions [23, 28, 25], acquiring additional environment data [21, 40], or leveraging inductive biases in representing states [51, 30, 37, 12, 12, 36] and actions [50, 47, 12]. What these algorithm-centric works overlook is that changing the data can be as or more effective for policy learning than changing the algorithm. In prior data-centric methods, the goal is usually to maximize *state diversity* through shared control [45, 44, 16, 27, 31, 35, 46], noise injection [33], or active queries [15, 6, 41, 29]. By only focusing on state coverage, these works are missing the role that actions (i.e., the expert) plays in the quality of data. A more complete understanding of data quality that integrates both state and action quality would not only improve performance but also save countless hours of data collection.

To better understand the role of both states and actions in the data for learning good policies, consider a single state transition — the three core factors that affect distribution shift are: the policy action distribution, the the stochasticity of transitions, and the previous state distribution. Note that the previous states are also just a function of the policy and dynamics back through time. Through this we extract two fundamental properties that can influence data quality in IL: *action divergence* and *transition diversity*. Action divergence captures how different the learned policy action distribution is from the expert’s actions at a given state: for example, if the expert is very consistent but the policy has high variance, then action divergence will be high and distribution shift is likely. Transition diversity captures the inherent variability of the environment at each state, which determines how the state distribution evolves for a given policy: for example, noisy dynamics in the low data regime can reduce overlap between the expert data and the learned policy distribution. Importantly, these factors can compound over time, thus greatly increasing the potential for distribution shift. While state coverage has been discussed in prior work, we are the first work to formalize the roles of both state and action distributions in data quality, along with how they interact through time: this new data-focused framing leads to insights about how to curate data to learn more effective policies.

To validate and study these properties empirically, we conduct two sets of experiments: (1) Data Noising, where we ablate these properties in robotics datasets to change the policy success rates, and (2) Data Measuring, where we observe human and machine generated datasets and approximately measure these properties in relationship to the policy success rates. Both experiments show that how state diversity, a commonly used heuristic for quality in prior work, is not always correlated with success. Furthermore, we find that in several human generated datasets, less consistent actions at each state is often associated with decreases in policy performance.

2 Related Work

Data quality research dates back to the early time of computing and the full literature is out of the scope of this paper. Existing literature in machine learning has proposed different dimensions of data quality including accuracy, completeness, consistency, timeliness, and accessibility [32, 14, 20]. We could draw similarities between action divergence with the concept of data consistency, and state diversity with completeness. However, instantiation of these metrics is non-trivial and domain-specific.

Our work is closely related to the imitation learning literature that explicitly addresses the distribution shift problem in various ways. Prior work can be divided into two camps: ones that take an *algorithm-centric* approach to account for biases in the dataset, and ones that employ *data-centric* methods for modifying the data collection process.

Algorithm-centric. Robust learning approaches including model-based imitation learning methods learn a dynamics model of the environment and therefore can plan to go back in distribution when the agent visits out of distribution states [21, 40]. Data augmentation is a useful post-processing technique when one could impose domain or task specific knowledge [23, 28, 25]. Prior work has also investigated how to explicitly learn from sub-optimal demonstrations by learning a weighting function over demonstrations either to guide BC training [9, 3] or as a reward function for RL algorithms [7, 11]. These methods either require additional information such as rankings of trajectories [9], demonstrator identity [3], or collecting additional environment data [7, 11]. Recent efforts on demonstration retrieval augment limited task-specific demonstrations with past robot experiences [38]. A recent

body of work build better inductive biases into the model for learning robust state features, like pretrained vision or language representations [51, 30, 37, 12]. Some approaches modify the action representation to be more expressive to capture all the expert’s actions, for example using Gaussian or mixture model action spaces [12, 36]. Others consider temporally abstracted action spaces like waypoints or action sequences to reduce the effective task length and thus mitigate compounding errors [50, 47, 12]. What these algorithm-centric works overlook is that changing the data can be as or more effective for policy learning than changing the algorithm. However, we still lack a comprehensive understanding of what properties in the data matter in imitation learning.

Data-centric. In more data-centric prior works that discuss data quality, the primary goal is often just to maximize state diversity. A large body of research focuses on modifying the data collection process such that the expert experience a diverse set of states. Ross et al. [45] proposed to iteratively collect *on-policy* demonstration data with shared-control between the expert and the robot, randomly switching with a gradually decreasing weight on the expert’s input, such that the training data contains direct samples of the expert policy at states experienced by the learned policy. However, randomly switching the control can make it unnatural for the human demonstrator and leads to noisier human control. To mitigate this issue, methods have been proposed to gate the control more effectively by evaluating metrics such as state uncertainty and novelty [16, 27]. Other methods allow the human to gate the control and effectively correct the robot’s behavior only when necessary [31, 35, 24, 46]. Closely related to our work, Laskey et al. [33] takes an optimal control perspective and showed that injecting control noise during data collection can give similar benefits as DAgger-style iterative methods. Active learning methods have also been developed to guide data collection towards more informative samples [15, 6, 41, 29]. By only focusing on state coverage, these works are missing the role that actions (i.e., the expert) plays in the quality of data.

3 Preliminaries

In imitation learning (IL), we assume access to a dataset $\mathcal{D}_N = \{\tau_1, \dots, \tau_N\}$ of N expert demonstrations. Each demonstration τ_i consists of a sequence of state-action pairs of length T_i , $\tau_i = \{(s_1, a_1), \dots, (s_{T_i}, a_{T_i})\}$, with states $s \in \mathcal{S}$ and actions $a \in \mathcal{A}$. Demonstrations are generated by sampling actions from the expert policy π_E through environment dynamics $\rho(s'|s, a)$. The objective of imitation learning is to learn a policy $\pi_\theta : \mathcal{S} \rightarrow \mathcal{A}$ that maps states to actions. Standard behavioral cloning optimizes a supervised loss maximizing the likelihood of the state-action pairs in the dataset:

$$\mathcal{L}(\theta) = -\frac{1}{|\mathcal{D}_N|} \sum_{(s,a) \in \mathcal{D}_N} \log \pi_\theta(a|s), \quad (1)$$

which is optimizing the following objective under finite samples from the expert:

$$\mathbb{E}_{s \sim \rho_{\pi_E}(\cdot)} [D_{\text{KL}}(\pi_E(\cdot|s), \pi_\theta(\cdot|s))] = -\mathbb{E}_{s \sim \rho_{\pi_E}(\cdot), a \sim \pi_E(\cdot|s)} [\log \pi_\theta(a|s)] + C \quad (2)$$

The C term here captures the entropy of the expert state-action distribution, which is constant with respect to θ and thus it does not affect optimality of θ . $\rho_{\pi_E}(s)$ is the state visitation of the expert policy, defined for any policy π as follows:

$$\rho_\pi(s) = \frac{1}{T} \sum_{t=1}^H \rho_\pi^t(s) \quad (3)$$

$$\rho_\pi^t(s') = \int_{s,a} \rho_\pi^t(s, a, s') ds da = \int_{s,a} \pi(a|s) \rho(s'|s, a) \rho_\pi^{t-1}(s) ds da \quad (4)$$

3.1 Distribution Shift in IL

Behavioral cloning methods as in Eq. (2) often assume that the dataset distribution is a good approximation of the true expert policy distribution. In most applications, however, the learned policy is bound to experience novel states that were not part of the training data due to stochasticity of the environment dynamics and the learned policy. Herein lies the fundamental challenge with imitation learning, i.e., state *distribution shift* between training and test time. Consider the training sample (s, a, s') at timestep t in demonstration τ_i . If the learned policy outputs $\tilde{a} \sim \pi(\cdot|s)$ which has a small action error $\epsilon = \tilde{a} - a$, the new state at the next time step will also deviate: $\tilde{s}' \sim \rho(s'|s, a + \epsilon)$, which in turn affects the policy output at the next step. In practice, the change in next state can be

highly disproportionate to $\|\epsilon\|$, so small errors can quickly lead the policy out of the data distribution. Stochastic dynamics, for example system noise, can compound with the distribution shift caused by policy errors, and as we continue to execute for $T - t$ steps, both these factors can compound over time to pull the policy out of distribution, often leading to task failure.

We can address this distribution shift problem by minimizing the mismatch between state visitation distribution of a learned policy π and the state visitation distribution of an expert policy π_E under some f -divergence D_f :

$$J(\pi, \pi_E) = D_f(\rho_\pi(s), \rho_{\pi_E}(s)) \quad (5)$$

Next, we connect this distribution shift problem to the question of data quality.

3.2 Formalizing Data Quality

How can we define and measure the quality of a dataset \mathcal{D} in IL? In existing literature, data quality has been used interchangeably with either the proficiency level of the expert at the task or the coverage of state space. However, these notions of quality are loose and incomplete: for example, they do not explain what concretely makes an expert better or worse, nor do they consider how stochasticity in the transitions impacts state space coverage and thus downstream learning. Our goal is to more formally define a measure of quality so that we can then optimize these properties in our datasets.

We posit that a complete notion of dataset quality is one that minimizes distribution shift in Eq. (5). This suggests that we cannot discuss data quality in isolation. The notion of data quality is heavily tied to the algorithm A that leads to the learned policy π_A as well as the expert policy π_E . We thus formalize the quality of a dataset \mathcal{D}_N conditioned on the expert policy π_E that generates it along with a policy learning algorithm A , as the negative distribution shift of a learned policy under some f -divergence D_f :

$$Q(\mathcal{D}_N; \pi_E, A) = -D_f(\rho_{\pi_A}(s), \rho_{\pi_E}(s)), \text{ where } \pi_A = A(\mathcal{D}_N) \quad (6)$$

Here, π_A is the policy learned by algorithm A using dataset \mathcal{D}_N of size N , which is generated from demonstrator π_E . Note that quality is affected by several components: the choice in demonstrator, the choice of dataset size, and the algorithm. The choice of expert policy π_E changes the trajectories in \mathcal{D}_N (which in turn affects policy learning) along with the desired state distribution $\rho_{\pi_E}(s)$. The dataset size controls the amount of information about the expert state distribution present in the dataset: note that π_A should match $\rho_{\pi_E}(s)$, but A learns only \mathcal{D}_N not from the full $\rho_{\pi_E}(s)$. The algorithm controls how the data is processed to produce the final policy π_A and thus the visited distribution $\rho_{\pi_A}(s)$.

To optimize this notion of quality, we might toggle any one of these factors. Prior work has studied algorithm modifications at length [36, 51, 4], but few works study how π_E and the dataset \mathcal{D}_N should be altered to perform best for any given algorithm A . We refer to this as *data curation*. In practice we often lack full control over the choice of π_E , since this is usually a human demonstrator; still, we can often influence π_E , for example through prompting or feedback [24], or we can curate the dataset derived from π_E through filtering [19].

4 Properties of Data Quality

To identify properties that affect data quality in imitation learning, we can study how each state transition $(s, a, s') \in \mathcal{D}$ in the dataset affects the dataset quality in detail. As we defined in Eq. (6), the dataset quality relies on distribution shift given an expert policy π_E and an imitation learning policy π_A . This relies on the state visitation distribution $\rho_{\pi_A}^t(s)$, which based on Eq. (4) depends on three terms: $\pi_A(a|s)$, $\rho(s'|s, a)$, and $\rho_{\pi_A}^{t-1}(s)$. Intuitively, three clear factors emerge for managing distribution shift: how different the policy $\pi_A(a|s)$ is from the expert $\pi_E(a|s)$ – which we refer to as *action divergence*, how diverse the dynamics $\rho(s'|a, s)$ are – which we refer to as *transition diversity*, and how these factors interact over time to produce past state visitation distribution $\rho_{\pi_A}^{t-1}(s)$. Importantly, the past state visitation can be controlled through *action divergence* and *transition diversity* at previous time steps, so in this section, we will formalize these two properties and discuss their implication on data curation.

4.1 Action Divergence

Action divergence is a measure of distance between the learned policy and the expert policy $D_f(\pi_A(\cdot|s), \pi_E(\cdot|s))$. This can stem from biases in the algorithm or dataset such as mismatched

action representations or lack of samples. While this is typically viewed in prior work as a facet of the algorithm or dataset size, importantly action divergence and thus data quality can also be influenced by the expert policy itself. For example, if the demonstrator knows the action representation used by the learning agent *a priori*, then the policy mismatch can be reduced by taking actions that are consistent with that action space. In [Theorem 4.1](#)¹, we illustrate the importance of action divergence by showing that our notion of data quality is lower bounded by the action divergence under the visited state distribution.

Theorem 4.1. *Given a policy π_A and demonstrator π_E and environment horizon length H , the distribution shift:*

$$D_{KL}(\rho_{\pi_A}, \rho_{\pi_E}) \leq \frac{1}{H} \sum_{t=0}^{H-1} (H-t) D_{KL}^{\rho_{\pi_A}^t}(\pi_A(\cdot|s), \pi_E(\cdot|s))$$

When using KL divergence for distribution shift in [Eq. \(5\)](#), we can see how the quality is lower bounded by the policy action divergence from the optimal policy under the visited state distribution, weighted at each step by time-to-go. Many prior works have noted the compounding error problem [\[45, 44\]](#), and here too action divergence at earlier timesteps has an out-sized effect on the overall distribution shift. Thus to optimize for the quality of a dataset, we should reduce the aggregated policy mismatch across visited trajectories.

Optimality: Many prior ideas around the “optimality” of a demonstration are intimately related to this action divergence property. Suboptimality that are naturally present in demonstrations like pauses or other action noise have been a source of difficulty when learning imitation policies [\[34, 4\]](#). These factors make it harder for the model to learn the expert action distributions, thus increasing action divergence. Suboptimality can also come from multi-modal expert policy distributions, and more expressive policy representations (i.e., reducing action divergence between the expert and the policy) has been shown to help [\[17, 12, 24\]](#). The speed of demonstration is another common notion of optimality, which decreases total action divergence by reducing horizon length H , provided it does not increase the per time step action divergence to compensate.

State Visitation: Critically, the visitation distribution in [Theorem 4.1](#) determines *where* action divergence should be low, whereas in the standard BC objective in [Eq. \(2\)](#), the divergence is only minimized under samples from the expert distribution $\rho_{\pi_E}^t$. To better understand how the visitation distribution evolves, we now analyze state transitions in greater detail.

4.2 Transition Diversity

Transition diversity encompasses the diversity of next state transitions seen at a given state for a certain policy. What role does transition diversity play in minimizing distribution shift? Intuitively, if we consider the upper bound in [Theorem 4.1](#), the expert’s state coverage should overlap as much as possible with the visited state distribution, but without increasing the action divergence.

Lemma 4.2. *Given a learned policy π_A and an expert policy π_E , assume that the policy is learned such that when $s \in \text{supp}(\rho_{\pi_E}^t)$, $D_{KL}(\pi_A(\cdot|s), \pi_E(\cdot|s)) \leq \beta$. Then:*

$$\begin{aligned} \mathbb{E}_{s \sim \rho_{\pi_A}^t} [D_{KL}(\pi_A(\cdot|s), \pi_E(\cdot|s))] &\leq \mathbb{E}_{s \in \rho_{\pi_A}^t} [\beta \mathbb{1}(s \in \text{supp}(\rho_{\pi_E}^t))] \\ &\quad + \mathbb{1}(s \notin \text{supp}(\rho_{\pi_E}^t)) D_{KL}(\pi_A(\cdot|s), \pi_E(\cdot|s)) \end{aligned}$$

[Lemma 4.2](#) shows that with a good learning algorithm (i.e., when β is small), it is important to maximize the overlap between the visited policy and the expert data (minimizes the contribution of the unbounded right term), but as shown in [Theorem 4.1](#) this should not come at the expense of increasing the action divergence of the policy. Rather than broadly maximizing state diversity, as prior works do, a more sensible approach is for the expert to maximize the two other factors that affect $\rho_{\pi_A}^t$: *system noise* and *initial state variance* in the expert data.

Finite Data and Low Coverage: While the above analysis holds for infinite data, maximizing transition diversity can lead to thinly spread coverage in the finite data regime. To analyze the finite data regime in isolation, we consider Gaussian system noise for simplicity. First, we formulate an empirical estimate of state “coverage” of the expert (i.e. the deviation from states in the expert

¹Proof for all theorems and lemmas in [Appendix A](#)

dataset). We then show that higher system noise can cause the learned policy π_A to deviate more from states sampled in the dataset.

Definition 1. For a given start state s , define the next state coverage probability over N samples from π_E for tolerance ϵ as $P_S(s; N, \epsilon) := P(\min_{i \in \{1 \dots N\}} \|s' - s'_{*,i}\|_\infty \leq \epsilon)$, where $\{s'_{*,i} \sim \rho_{\pi_E}^t(\cdot|s)\}$ is a set of N sampled next state transitions under the expert policy π_E starting at s , and $s' \sim \rho_{\pi_A}^t(\cdot|s)$ is a sampled next state under the policy π_A starting at S .

We can think of $P_S(s; N, \epsilon)$ as the probability under potential datasets for π_E of seeing a next state at test time (under π_A) that was nearby the next states in the dataset, conditioned at a starting state s (i.e., coverage). This is related to a single step of distribution shift, but measured over a dataset rather than a distribution. Defining coverage as the distance to the dataset being below some threshold is reasonable for function approximators like neural networks [2].

Theorem 4.3. Given a policy π_A and demonstrator π_E , assume that for state s , if $\rho_{\pi_E}^{t-1}(s) > 0$, then $\pi_A(a|s) = \pi_E(a|s)$. Assume that transitions are normally distributed with fixed and diagonal variance, $\rho(s'|s, a) = \mathcal{N}(\mu(s, a), \sigma^2 I)$, then the next state coverage probability is $P_S(s; N, \epsilon) = 1 - (1 - \text{erf}(\frac{\epsilon}{2\sigma})^d)^N$, where d is the dimensionality of the state.

In [Theorem 4.3](#), we see that even under a policy that is perfect when in distribution, the probability of next state coverage decreases as the variance of system noise σ^2 increases, for a fixed sampling budget N . However, increasing N has a much stronger positive effect on coverage than decreases in σ , suggesting that system noise is only an issue when the dataset size is sufficiently small. Furthermore, ϵ here represents some simplistic form of the *generalization* capacity of the policy, and we see here that increasing ϵ makes us more robust to proportional increases in σ .

Finite Data and Good Coverage: However, if we assume N is large enough to mitigate the coverage effect of system noise, are there any other effects of transition diversity in the dataset? The answer lies in generalization properties of the algorithm, which as provided in [Theorem 4.3](#) are fairly conservative (i.e., in the definition of $P_S(s; N, \epsilon)$). In [Theorem A.1](#) in [Appendix A](#), we use a more loose generalization definition and relax the assumption that the learned policy is perfect. We show as system noise increases, the resulting boost in sample coverage can actually replicate and overcome the effects of high learned policy noise, suggesting that more system noise can actually be beneficial for learning. This finding sheds light on results from prior work and our own experiments in [Section 5](#) that show the benefits of collecting data in the presence of high system noise [33]. Plots of both coverage probabilities for different N are included in [Appendix A](#).

4.3 Implications for Data Curation

We have shown how action divergence and transition diversity are both tied to distribution shift and thus data quality. Based on action divergence and transition diversity, we now examine downstream implications of these properties on what matters for *data curation*, where the goal is to collect and then select *high quality* demonstrations in our dataset \mathcal{D}_N for good policy learning.

Action Consistency: To minimize action divergence, the algorithm action representation should *align* with the expert’s action distribution, for the given dataset size. One algorithmic solution is to improve the expressiveness of the policy action space so it can capture the exact actions at every state that was demonstrated. However, in practice, individual states might only be visited a few times in the dataset, and so if the entropy of the expert policy at those states is high, the learned policy will find it difficult to perfectly match the actions even for the most expressive action spaces. Instead, we argue that expert data should be curated to have more *consistent* actions, e.g., reducing the entropy of the expert policy: $\mathbb{E}_{s \sim \rho_{\pi_A}(\cdot)}[\mathcal{H}(\pi_E(\cdot|s))]$. Since knowing the visited state distribution is impossible beforehand, the best we can do is to encourage low entropy in the expert data distribution:

$$\min_{\pi_E} \mathbb{E}_{s \sim \rho_{\pi_E}(\cdot)}[\mathcal{H}(\pi_E(\cdot|s))] \tag{7}$$

State Diversity: As discussed previously, the state visitation of the policy depends on the trajectory action distribution, the initial state distribution, and the system noise distribution. Many prior works seek to improve the *state coverage* of the dataset, using some metric similar to [Definition 1](#) [6, 29]. However, the required state diversity is a function of the learned policy mismatch (action divergence) and the noise present in the system (transition diversity), and is thus a coarse representation of data quality. Uniformly increasing coverage over the state space is not necessarily a good thing — as shown in [Section 4.1](#), if state coverage comes at the expense of action consistency, the result might

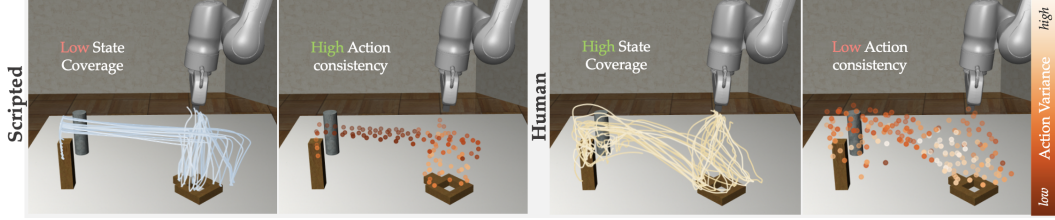


Figure 1: **Case Study:** Trajectories and action variance for scripted (left two plots) compared to human demonstration data (right two plots). Even though the human data (right) has high state coverage, the action variance is high, leading to high action divergence, and vice versa.

be worse than a policy trained on less state coverage but more consistent actions. Instead, we argue that we should optimize for system noise.

System Noise: Although system noise at a given state cannot be controlled, experts can control system noise at the trajectory level (e.g. visiting states with more or less system noise). Should system noise be encouraged or discouraged in a dataset? Based on the discussion in Section 4.2, we hypothesize that when the dataset size is fixed, increasing the system noise can increase the *coverage* of the expert and thus improve robustness in the learned policy (Theorem A.1), but only up to a certain point, when the data becomes too sparse to generalize (Theorem 4.3). Thus, in addition to consistent actions, we posit that expert demonstrators should encourage paths with high system entropy for learning better policies, such that the overall state entropy stays below some threshold γ to avoid coverage that is too sparse.

$$\begin{aligned} \max_{\pi_E} \mathbb{E}_{s \sim \rho_{\pi_E}(\cdot), a \sim \pi_E(\cdot|s)} [\mathcal{H}(\rho(\cdot|a, s))] \\ \text{s.t. } H(\rho_{\pi_E}(s)) \leq \gamma \end{aligned} \quad (8)$$

Horizon Length: The length of trajectories in the expert data also can have a large effect on the expert and visited state distributions, and thus on the quality of the dataset. However, while horizon length certainly plays a role, like state diversity, it is a downstream effect of action divergence and transition diversity. Based on previous analysis, what really matters is minimizing the *aggregated* action divergence and transition diversity produced by the expert demonstrator across time. Horizon length alone only crudely measures this, but is often correlated in practice as we show in Section 5.2.

While prior work in data curation primarily aim to maximize state diversity alone, our analysis of data quality reveals several new properties that matter for data curation, such as action consistency, system noise, and their combined effect over time. As we demonstrate in the next section, understanding these properties and the inherent tradeoffs between them is vital for data curation in imitation learning.

5 Analysis

To empirically analyze how different data properties affect imitation learning, we conduct two sets of experiments. In the first set, we generate various quality expert datasets by adding different types of noise to *scripted* policies, i.e., policies that are hand-designed to be successful at the task. An example scripted policy compared to human demonstrations is shown in Fig. 1. We study both noise in the system – considering transition diversity – and noise added to the expert policy – considering both transition diversity and action divergence – as a function of dataset size. In the second set of experiments, we evaluate the empirical properties (see Appendix B) for real human collected datasets.

5.1 Data Noising

We train Behavior Cloning (BC) with data generated with system noise and policy noise in two environments: *PMObstacle*, a 2D environment where a point mass agent must reach a target point without hitting an obstacle in its way; and *Square*, a 3D environment where a robot arm must pick up a square nut and insert it onto a peg (shown in Fig. 1). In both, system and policy noise are Gaussian random variables added to the dynamics and scripted policy, respectively, at each time step, and BC uses an MLP architecture. Fig. 2 shows results in *PMObstacle* (top row) and *Square* (bottom row).

State Diversity through Transition Diversity improves performance, up to a point. The left plots in Fig. 2 (a)-(d) show policy success rates as we vary system noise (σ_s) (more noise for lighter color

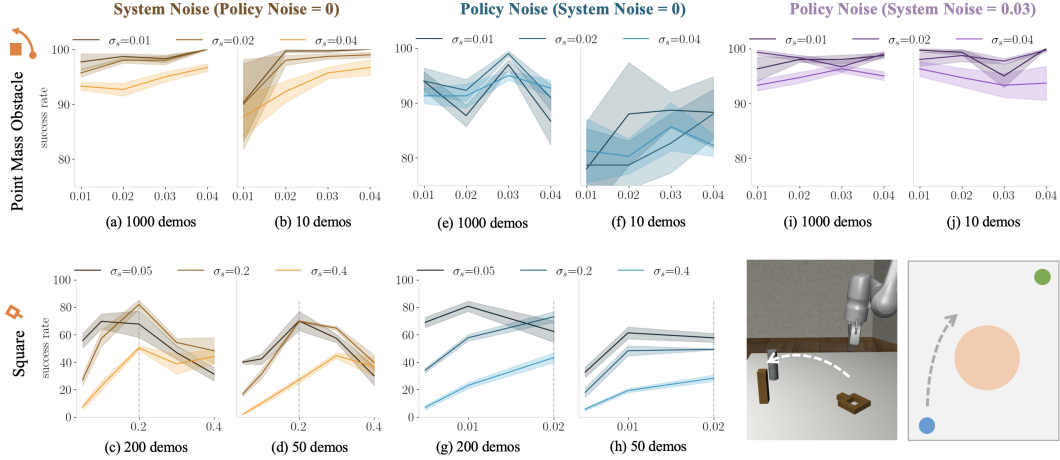


Figure 2: BC Success rates in *PMObstacle* (top row) for 1000 and 10 episodes of data, and in *Square* (bottom row) for 200 and 50 episodes of data (error bars over 3 datasets). X-axis corresponds to injected Gaussian noise in the *dataset* and each line corresponds to injected system noise (σ_s) during *evaluation*. **System Noise** (left): for large datasets (a)(c), higher system noise during evaluation decreases performance, but more system noise during training does the best. For small datasets (b)(d), we note a similar but exaggerated effect. **Policy Noise** (mid) For large datasets (e)(g), unlike system noise, more expert policy noise often hurts performance despite similar state coverage. For small datasets (f)(h), adding policy noise exaggerates this effect and produces large variance in performance. For *Square*, the dotted lines mark comparable values of noise in terms of state coverage. **System + Policy Noise** (i)(j): Adding some system noise can make the policy more robust to action divergence.

shades), where (a)(c) show the high-data regime and the (b)(d) show the low data regime. Higher system noise tends to improve policy performance in the high data regime, but only up to a point for *Square* — after $\sigma_s = 0.3$ in the expert data (c), performance starts to drop off, which we hypothesize is due to the low coverage, based on the analysis of transition diversity in Section 4.2. In the low data regime, the story is similar but even more exaggerated, with increasing system noise leading to comparable performance as the high data regime. Once again for *Square*, increasing transition diversity (d) helps until the state coverage is too thin. See Table 2, Table 5, and Table 6 in Appendix C for the full sweep of system noise values in each environment.

State Diversity at the cost of Action Divergence hurts performance. Plots in Fig. 2 (e)(f) and Fig. 2 (i)(j) show policy success rates for increasing the policy noise (σ_p) in the dataset, where the (e)(g) show the high data regime and the (f)(h) show the low data regime. Note that each value of policy noise yields the same expert state distribution as the corresponding amount of system noise. Since this noise is zero-mean and the learned policy is deterministic, policy noise in the high data regime (e)(g) is only moderately worse as compared to equivalent amounts of system noise (a)(c), suggesting that the action divergence is minor. In fact, due to the added state diversity, adding policy noise in the high data regime helps up to a certain point. However in the low data regime (f)(h), performance is substantially worse compared to comparable system noise, since the policy can not recover the unbiased expert policy from just a few noisy examples (note that in (c)(d), the x-axes are not aligned with those in (g)(h), and $\sigma_s = 0.2$ corresponds to $\sigma_p = 0.02$ as shown by the dotted line). This illustrates that state diversity coming from the noise in the expert policy can increase action divergence, and thus high state diversity is not universally desirable. See Table 3, Table 7, and Table 8 in Appendix C for the full sweep of policy noise values in each environment.

Transition Diversity can counteract the effects of policy noise. In the right two plots (i)(j) for *PMObstacle* in Fig. 2, the dataset combines both system and policy noise. The system noise is fixed ($\sigma_s = 0.03$) and the policy noise is varied in the same range as the middle two plots (just policy noise). Given the analysis in Section 4.2 and Theorem A.1 in Appendix A, we would expect that having some system noise could actually make the policy much more robust to policy noise, since the state coverage provided in the dataset can help learn a more robust policy (generalization). Indeed we find that just by adding system noise, the learned policy becomes very robust to added policy noise in both the high (i) and low (j) regimes. This suggests that adding transition diversity can help mitigate the affects of action divergence incurred by noisy or sub-optimal experts. See Table 4 in Appendix C for the full sweep of policy noise values for fixed system noise in each environment.

5.2 Data Measuring

Next we empirically instantiate several metrics from [Section 4.3](#) that capture various facets of data quality, and measure different datasets: (1) action variance (higher means less action consistency) measured through clustering nearby states (2) horizon length H (higher means longer trajectories), and (3) state similarity (opposite of state diversity) measured as the average cluster size. See [Appendix B](#) for the exact empirical definitions. We leave out system noise since these human datasets were collected in deterministic environments.

In [Table 1](#), we consider single and multi-human datasets from the *Square* and *Can* tasks from robomimic [\[36\]](#). We see that higher action variance and horizon length are often accompanied by decreases in success rates. The *Worse* multi-human datasets have seemingly lower action variance but less state similarity, and yet qualitatively we observed highly multi-modal behaviors in these datasets (e.g., grasping different parts of the nut instead of the handle). We suspect that this type of multi-modality is not measured well by the single time step action variance metric, but rather requires a longer term view of the effects of that action on the scene – as indicated in [Theorem 4.1](#). Additionally, state diversity once again is not correlated with performance on the task.

	<i>Square</i>				<i>Can</i>			
	PH	Better	Okay	Worse	PH	Better	Okay	Worse
Success Rate	58	36	12	2	96	56	40	22
Dataset Size (N)	200	100	100	100	200	100	100	100
Action Variance	0.073	0.062	0.099	0.061	0.051	0.066	0.079	0.063
Horizon Length (H)	150	190	250	350	115	140	180	300
State Similarity	8.2e-5	1.8e-4	1.7e-4	1.2e-4	1.0e-4	2.1e-4	2.4e-4	2.0e-4

Table 1: Data Quality metrics evaluated on *Square* (left) and *Can* (right) for proficient human (PH), and multi human (Better, Okay, Worse) datasets. PH and Better overlap in some of the data.

We emphasize that these metrics likely do not provide a complete picture of data quality, but they do provide us insights into why performance is low and how data collection can be improved in future datasets. Through future efforts from the community, we envision a comprehensive set of data metrics that practitioners can use to quickly evaluate the quality of datasets without needing to first train and evaluate models on those datasets.

6 Discussion

Data curation is incredibly important for maximizing the potential of any given algorithm, and especially so in imitation learning. To curate data, one needs to establish a formalism for assessing data quality. The predominant notions of data quality today are solely centered around maximizing *state diversity* in a dataset, which ignore the quality of the expert’s demonstrated actions and how these factors interplay. In this work, we propose a holistic view of data curation centered around minimizing distribution shift. We demonstrate that action divergence and transition diversity are crucial factors in data quality that can often be controlled or measured, and we draw several valuable insights from this shedding light on effective strategies for curating expert datasets. We find that making actions more consistent tends to increase policy success. Furthermore, we observe a fundamental tradeoff between state diversity and action divergence — increasing state diversity can often come at the expense of action divergence. Instead of uniformly maximizing state diversity, we show that increasing transition diversity improves performance until the data coverage becomes too sparse. While the metrics presented in our experiments are often good measures of final performance, we find that comprehensively measuring data quality in practice for real world datasets can be quite challenging. Finally, we envision a broader set of metrics informed by our formalism for data quality that practitioners can use to curate datasets, and we believe our work is an important first step in formulating and evaluating these metrics.

References

[1] Abubakar Abid, Maheen Farooqi, and James Zou. Large language models associate muslims with violence. *Nature Machine Intelligence*, 3(6):461–463, 2021.

- [2] Jonathan Baxter. A model of inductive bias learning. *Journal of artificial intelligence research*, 12:149–198, 2000.
- [3] Mark Beliaev, Andy Shih, Stefano Ermon, Dorsa Sadigh, and Ramtin Pedarsani. Imitation learning by estimating expertise of demonstrators. In *International Conference on Machine Learning*, pages 1732–1748. PMLR, 2022.
- [4] Suneel Belkhale and Dorsa Sadigh. Plato: Predicting latent affordances through object-centric play. In *6th Annual Conference on Robot Learning*, 2022.
- [5] Federico Bianchi, Pratyusha Kalluri, Esin Durmus, Faisal Ladhak, Myra Cheng, Debora Nozza, Tatsunori Hashimoto, Dan Jurafsky, James Zou, and Aylin Caliskan. Easily accessible text-to-image generation amplifies demographic stereotypes at large scale. *ACM Conference on Fairness, Accountability, and Transparency*, 2023.
- [6] Erdem Bıyık, Malayandi Palan, Nicholas C Landolfi, Dylan P Losey, and Dorsa Sadigh. Asking easy questions: A user-friendly approach to active reward learning. *arXiv preprint arXiv:1910.04365*, 2019.
- [7] Daniel S Brown, Wonjoon Goo, and Scott Niekum. Better-than-demonstrator imitation learning via automatically-ranked demonstrations. In *Conference on robot learning*, pages 330–359. PMLR, 2020.
- [8] Tom Brown, Benjamin Mann, Nick Ryder, Melanie Subbiah, Jared D Kaplan, Prafulla Dhariwal, Arvind Neelakantan, Pranav Shyam, Girish Sastry, Amanda Askell, et al. Language models are few-shot learners. *Advances in neural information processing systems*, 33:1877–1901, 2020.
- [9] Zhangjie Cao, Zihan Wang, and Dorsa Sadigh. Learning from imperfect demonstrations via adversarial confidence transfer. In *2022 International Conference on Robotics and Automation (ICRA)*, pages 441–447. IEEE, 2022.
- [10] Ting-Yun Chang and Robin Jia. Careful data curation stabilizes in-context learning, 2022.
- [11] Letian Chen, Rohan Paleja, and Matthew Gombolay. Learning from suboptimal demonstration via self-supervised reward regression. In *Conference on robot learning*, pages 1262–1277. PMLR, 2021.
- [12] Cheng Chi, Siyuan Feng, Yilun Du, Zhenjia Xu, Eric Cousineau, Benjamin Burchfiel, and Shuran Song. Diffusion policy: Visuomotor policy learning via action diffusion. In *Proceedings of Robotics: Science and Systems (RSS)*, 2023.
- [13] Aakanksha Chowdhery, Sharan Narang, Jacob Devlin, Maarten Bosma, Gaurav Mishra, Adam Roberts, Paul Barham, Hyung Won Chung, Charles Sutton, Sebastian Gehrmann, et al. Palm: Scaling language modeling with pathways. *arXiv preprint arXiv:2204.02311*, 2022.
- [14] Corinna Cichy and Stefan Rass. An overview of data quality frameworks. *IEEE Access*, 7: 24634–24648, 2019.
- [15] Yuchen Cui and Scott Niekum. Active reward learning from critiques. In *2018 IEEE international conference on robotics and automation (ICRA)*, pages 6907–6914. IEEE, 2018.
- [16] Yuchen Cui, David Isele, Scott Niekum, and Kikuo Fujimura. Uncertainty-aware data aggregation for deep imitation learning. In *2019 International Conference on Robotics and Automation (ICRA)*, pages 761–767. IEEE, 2019.
- [17] Zichen Jeff Cui, Yibin Wang, Nur Muhammad Mahi Shafiullah, and Lerrel Pinto. From play to policy: Conditional behavior generation from uncurated robot data. In *International Conference on Learning Representations*, 2023. URL <https://openreview.net/forum?id=c7rM7F7jQjN>.
- [18] Alexey Dosovitskiy, Lucas Beyer, Alexander Kolesnikov, Dirk Weissenborn, Xiaohua Zhai, Thomas Unterthiner, Mostafa Dehghani, Matthias Minderer, Georg Heigold, Sylvain Gelly, et al. An image is worth 16x16 words: Transformers for image recognition at scale. In *International Conference on Learning Representations*, 2020.

- [19] Maximilian Du, Suraj Nair, Dorsa Sadigh, and Chelsea Finn. Behavior retrieval: Few-shot imitation learning by querying unlabeled datasets. In *Proceedings of Robotics: Science and Systems (RSS)*, 2023.
- [20] Lisa Ehrlinger and Wolfram Wöb. A survey of data quality measurement and monitoring tools. *Frontiers in big data*, page 28, 2022.
- [21] Peter Englert, Alexandros Paraschos, Marc Peter Deisenroth, and Jan Peters. Probabilistic model-based imitation learning. *Adaptive Behavior*, 21(5):388–403, 2013.
- [22] Hugging Face. Starcoder. <https://github.com/bigcode-project/starcoder>, 2023.
- [23] Alexandre Galashov, Josh S Merel, and Nicolas Heess. Data augmentation for efficient learning from parametric experts. *Advances in Neural Information Processing Systems*, 35:31484–31496, 2022.
- [24] Kanishk Gandhi, Siddharth Karamcheti, Madeline Liao, and Dorsa Sadigh. Eliciting compatible demonstrations for multi-human imitation learning. In *Proceedings of the 6th Conference on Robot Learning (CoRL)*, 2022.
- [25] Pierre-Louis Guhur, Shizhe Chen, Ricardo Garcia Pinel, Makarand Tapaswi, Ivan Laptev, and Cordelia Schmid. Instruction-driven history-aware policies for robotic manipulations. In *Conference on Robot Learning*, pages 175–187. PMLR, 2023.
- [26] Kaiming He, Xinlei Chen, Saining Xie, Yanghao Li, Piotr Dollár, and Ross Girshick. Masked autoencoders are scalable vision learners. In *Proceedings of the IEEE/CVF Conference on Computer Vision and Pattern Recognition*, pages 16000–16009, 2022.
- [27] Ryan Hoque, Ashwin Balakrishna, Ellen Novoseller, Albert Wilcox, Daniel S Brown, and Ken Goldberg. Thriftydagger: Budget-aware novelty and risk gating for interactive imitation learning. In *Conference on Robot Learning*, pages 598–608. PMLR, 2022.
- [28] Stephen James and Andrew J Davison. Q-attention: Enabling efficient learning for vision-based robotic manipulation. *IEEE Robotics and Automation Letters*, 7(2):1612–1619, 2022.
- [29] Hong Jun Jeon, Smitha Milli, and Anca D Dragan. Reward-rational (implicit) choice: A unifying formalism for reward learning. In *Conference on Neural Information Processing Systems*, 2020.
- [30] Siddharth Karamcheti, Suraj Nair, Annie S Chen, Thomas Kollar, Chelsea Finn, Dorsa Sadigh, and Percy Liang. Language-driven representation learning for robotics. In *Proceedings of Robotics: Science and Systems (RSS)*, 2023.
- [31] Michael Kelly, Chelsea Sidrane, Katherine Driggs-Campbell, and Mykel J Kochenderfer. Hg-dagger: Interactive imitation learning with human experts. In *2019 International Conference on Robotics and Automation (ICRA)*, pages 8077–8083. IEEE, 2019.
- [32] Nuno Laranjeiro, Seyma Nur Soydemir, and Jorge Bernardino. A survey on data quality: classifying poor data. In *2015 IEEE 21st Pacific rim international symposium on dependable computing (PRDC)*, pages 179–188. IEEE, 2015.
- [33] Michael Laskey, Jonathan Lee, Roy Fox, Anca Dragan, and Ken Goldberg. Dart: Noise injection for robust imitation learning. In *Conference on robot learning*, pages 143–156. PMLR, 2017.
- [34] Corey Lynch, Mohi Khansari, Ted Xiao, Vikash Kumar, Jonathan Tompson, Sergey Levine, and Pierre Sermanet. Learning latent plans from play. In *Conference on robot learning*, pages 1113–1132. PMLR, 2020.
- [35] Ajay Mandlekar, Danfei Xu, Roberto Martín-Martín, Yuke Zhu, Li Fei-Fei, and Silvio Savarese. Human-in-the-loop imitation learning using remote teleoperation. *arXiv preprint arXiv:2012.06733*, 2020.
- [36] Ajay Mandlekar, Danfei Xu, Josiah Wong, Soroush Nasiriany, Chen Wang, Rohun Kulkarni, Li Fei-Fei, Silvio Savarese, Yuke Zhu, and Roberto Martín-Martín. What matters in learning from offline human demonstrations for robot manipulation. *arXiv preprint arXiv:2108.03298*, 2021.

- [37] Suraj Nair, Aravind Rajeswaran, Vikash Kumar, Chelsea Finn, and Abhinav Gupta. R3m: A universal visual representation for robot manipulation. In *6th Annual Conference on Robot Learning*, 2022. URL <https://openreview.net/forum?id=tGbpzg6y0rI>.
- [38] Soroush Nasiriany, Tian Gao, Ajay Mandlekar, and Yuke Zhu. Learning and retrieval from prior data for skill-based imitation learning. In *6th Annual Conference on Robot Learning*, 2022.
- [39] Xu Ouyang, Shahina Mohd Azam Ansari, Felix Xiaozhu Lin, and Yangfeng Ji. Efficient model finetuning for text classification via data filtering, 2022.
- [40] Carl Qi, Pieter Abbeel, and Aditya Grover. Imitating, fast and slow: Robust learning from demonstrations via decision-time planning. *arXiv preprint arXiv:2204.03597*, 2022.
- [41] Mattia Racca, Antti Oulasvirta, and Ville Kyrki. Teacher-aware active robot learning. In *2019 14th ACM/IEEE International Conference on Human-Robot Interaction (HRI)*, pages 335–343. IEEE, 2019.
- [42] Alec Radford, Jong Wook Kim, Chris Hallacy, Aditya Ramesh, Gabriel Goh, Sandhini Agarwal, Girish Sastry, Amanda Askell, Pamela Mishkin, Jack Clark, et al. Learning transferable visual models from natural language supervision. In *International conference on machine learning*, pages 8748–8763. PMLR, 2021.
- [43] Scott Reed, Konrad Zolna, Emilio Parisotto, Sergio Gomez Colmenarejo, Alexander Novikov, Gabriel Barth-Maron, Mai Gimenez, Yury Sulsky, Jackie Kay, Jost Tobias Springenberg, et al. A generalist agent. *arXiv preprint arXiv:2205.06175*, 2022.
- [44] Stéphane Ross and Drew Bagnell. Efficient reductions for imitation learning. In *Proceedings of the thirteenth international conference on artificial intelligence and statistics*, pages 661–668. JMLR Workshop and Conference Proceedings, 2010.
- [45] Stéphane Ross, Geoffrey Gordon, and Drew Bagnell. A reduction of imitation learning and structured prediction to no-regret online learning. In *Proceedings of the fourteenth international conference on artificial intelligence and statistics*, pages 627–635. JMLR Workshop and Conference Proceedings, 2011.
- [46] Mariah L Schrum, Erin Hedlund-Botti, Nina Moorman, and Matthew C Gombolay. Mind meld: Personalized meta-learning for robot-centric imitation learning. In *2022 17th ACM/IEEE International Conference on Human-Robot Interaction (HRI)*, pages 157–165. IEEE, 2022.
- [47] Mohit Shridhar, Lucas Manuelli, and Dieter Fox. Perceiver-actor: A multi-task transformer for robotic manipulation. In *6th Annual Conference on Robot Learning*, 2022.
- [48] Jonathan Spencer, Sanjiban Choudhury, Arun Venkatraman, Brian Ziebart, and J Andrew Bagnell. Feedback in imitation learning: The three regimes of covariate shift. *arXiv preprint arXiv:2102.02872*, 2021.
- [49] Romal Thoppilan, Daniel De Freitas, Jamie Hall, Noam Shazeer, Apoorv Kulshreshtha, Heng-Tze Cheng, Alicia Jin, Taylor Bos, Leslie Baker, Yu Du, et al. Lamda: Language models for dialog applications. *arXiv preprint arXiv:2201.08239*, 2022.
- [50] Tony Z. Zhao, Vikash Kumar, Sergey Levine, and Chelsea Finn. Learning fine-grained bimanual manipulation with low-cost hardware. In *Proceedings of Robotics: Science and Systems (RSS)*, 2023.
- [51] Yifeng Zhu, Abhishek Joshi, Peter Stone, and Yuke Zhu. Viola: Imitation learning for vision-based manipulation with object proposal priors. *6th Annual Conference on Robot Learning (CoRL)*, 2022.

A Theoretical Results

Theorem 4.1: For a discrete state space \mathcal{S} and action space \mathcal{A} , given a policy π_A and demonstrator π_E and environment horizon length H , the distribution shift $D_{\text{KL}}(\rho_{\pi_A}, \rho_{\pi_E}) \leq \frac{1}{H} \sum_{t=0}^{H-1} (H-t) D_{\text{KL}}^{s \sim \rho_{\pi_A}^t}(\pi_A(\cdot|s), \pi_E(\cdot|s))$

Proof. Using the log-sum inequality:

$$\begin{aligned}
D_{\text{KL}}(\rho_{\pi_A}^t, \rho_{\pi_E}^t) &= \int_{s'} \rho_{\pi_A}^t(s') \log \frac{\rho_{\pi_A}^t(s')}{\rho_{\pi_E}^t(s')} \\
&= \int_{s'} \left(\int_{s,a} \rho_{\pi_A}^{t-1}(s) \pi_A(a|s) \rho(s'|a, s) \right) \log \frac{\int_{s,a} \rho_{\pi_A}^{t-1}(s) \pi_A(a|s) \rho(s'|a, s)}{\int_{s,a} \rho_{\pi_E}^{t-1}(s) \pi_E(a|s) \rho(s'|a, s)} \\
&\leq \int_{s'} \int_{s,a} \rho_{\pi_A}^{t-1}(s) \pi_A(a|s) \rho(s'|a, s) \log \frac{\rho_{\pi_A}^{t-1}(s) \pi_A(a|s) \rho(s'|a, s)}{\rho_{\pi_E}^{t-1}(s) \pi_E(a|s) \rho(s'|a, s)} \\
&\leq \int_{s'} \int_{s,a} \rho_{\pi_A}^{t-1}(s) \pi_A(a|s) \rho(s'|a, s) \left(\log \frac{\rho_{\pi_A}^{t-1}(s)}{\rho_{\pi_E}^{t-1}(s)} + \log \frac{\pi_A(a|s)}{\pi_E(a|s)} \right) \\
&\leq \int_{s,a} \rho_{\pi_A}^{t-1}(s) \pi_A(a|s) \left(\log \frac{\rho_{\pi_A}^{t-1}(s)}{\rho_{\pi_E}^{t-1}(s)} + \log \frac{\pi_A(a|s)}{\pi_E(a|s)} \right) \\
&\leq \int_s \rho_{\pi_A}^{t-1}(s) \log \frac{\rho_{\pi_A}^{t-1}(s)}{\rho_{\pi_E}^{t-1}(s)} + \int_{s,a} \rho_{\pi_A}^{t-1}(s) \pi_A(a|s) \log \frac{\pi_A(a|s)}{\pi_E(a|s)} \\
&\leq D_{\text{KL}}(\rho_{\pi_A}^{t-1}, \rho_{\pi_E}^{t-1}) + D_{\text{KL}}^{s \sim \rho_{\pi_A}^t}(\pi_A(\cdot|s), \pi_E(\cdot|s)) \\
&\leq D_{\text{KL}}(\rho^0(\cdot), \rho^0(\cdot)) + \sum_{j=0}^{t-1} D_{\text{KL}}^{s \sim \rho_{\pi_A}^j}(\pi_A(\cdot|s), \pi_E(\cdot|s)) \quad \triangleright \text{Expanding recursively} \\
&\leq \sum_{j=0}^{t-1} D_{\text{KL}}^{s \sim \rho_{\pi_A}^j}(\pi_A(\cdot|s), \pi_E(\cdot|s)) \\
D_{\text{KL}}(\rho_{\pi_A}, \rho_{\pi_E}) &= \int_s \left(\frac{1}{H} \sum_{t=1}^H \rho_{\pi_A}^t(s) \right) \log \frac{\sum_{t=1}^H \rho_{\pi_A}^t(s)}{\sum_{t=1}^H \rho_{\pi_E}^t(s)} \\
&\leq \int_s \sum_{t=1}^H \rho_{\pi_A}^t(s) \log \frac{\rho_{\pi_A}^t(s)}{\rho_{\pi_E}^t(s)} \\
&\leq \frac{1}{H} \sum_{t=1}^H D_{\text{KL}}(\rho_{\pi_A}^t, \rho_{\pi_E}^t) \\
&\leq \frac{1}{H} \sum_{t=1}^H \sum_{j=0}^{t-1} D_{\text{KL}}^{s \sim \rho_{\pi_A}^j}(\pi_A(\cdot|s), \pi_E(\cdot|s)) \\
&\leq \frac{1}{H} \sum_{t=0}^{H-1} (H-t) D_{\text{KL}}^{s \sim \rho_{\pi_A}^t}(\pi_A(\cdot|s), \pi_E(\cdot|s))
\end{aligned}$$

□

Lemma 4.2: Given learned policy π_A and expert π_E , define assume that the policy is learned such that when $s \in \text{supp}(\rho_{\pi_E}^t)$, $D_{\text{KL}}(\pi_A(\cdot|s), \pi_E(\cdot|s)) \leq \beta$. Then $\mathbb{E}_{s \sim \rho_{\pi_A}^t} [D_{\text{KL}}(\pi_A(\cdot|s), \pi_E(\cdot|s))] \leq \mathbb{E}_{s \in \rho_{\pi_A}^t} [\beta \mathbb{1}(s \in \text{supp}(\rho_{\pi_E}^t)) + \mathbb{1}(s \notin \text{supp}(\rho_{\pi_E}^t)) D_{\text{KL}}(\pi_A(\cdot|s), \pi_E(\cdot|s))]$

Proof. This follows by simple substitution:

$$\begin{aligned} \mathbb{E}_{s \sim \rho_{\pi_A}^t} [D_{\text{KL}}(\pi_A(\cdot|s), \pi_E(\cdot|s))] &= \mathbb{E}_{s \in \rho_{\pi_A}^t} [\mathbb{1}(s \in \text{supp}(\rho_{\pi_E}^t)) D_{\text{KL}}(\pi_A(\cdot|s), \pi_E(\cdot|s)) \\ &\quad + \mathbb{1}(s \notin \text{supp}(\rho_{\pi_E}^t)) D_{\text{KL}}(\pi_A(\cdot|s), \pi_E(\cdot|s))] \\ &\leq \mathbb{E}_{s \in \rho_{\pi_A}^t} [\beta \mathbb{1}(s \in \text{supp}(\rho_{\pi_E}^t)) \\ &\quad + \mathbb{1}(s \notin \text{supp}(\rho_{\pi_E}^t)) D_{\text{KL}}(\pi_A(\cdot|s), \pi_E(\cdot|s))] \end{aligned}$$

□

Theorem 4.3: Given a policy π_A and demonstrator π_E , assume that for state s , if $\rho_{\pi_E}^{t-1}(s) > 0$, then $\pi_A(a|s) = \pi_E(a|s)$. Assume that transitions are normally distributed with fixed and diagonal variance, $\rho(s'|s, a) = \mathcal{N}(\mu(s, a), \sigma^2 I)$, then the next state coverage probability is $P_S(s; N, \epsilon) = 1 - (1 - \text{erf}(\frac{\epsilon}{2\sigma})^d)^N$, where d is the dimensionality of the state.

Proof. Since samples and dimensions are independent, we can decompose probabilities as follows:

$$\begin{aligned} P_S(s; N, \epsilon) &= P(\min_{i \in \{1 \dots N\}} \|s' - s'_{*,i}\|_{\infty} \leq \epsilon) \\ &= 1 - P(\min_{i \in \{1 \dots N\}} \|s' - s'_{*,i}\|_{\infty} > \epsilon) \\ &= 1 - \prod_{i=1}^N P(\|s' - s'_{*,i}\|_{\infty} > \epsilon) \\ &= 1 - \prod_{i=1}^N (1 - P(\|s' - s'_{*,i}\|_{\infty} \leq \epsilon)) \\ &= 1 - \prod_{i=1}^N \left(1 - \prod_{j=1}^d P(|s'[j] - s'_{*,i}[j]| \leq \epsilon) \right) \end{aligned}$$

The next state from the policy is $s' \sim \mathcal{N}(\mu(s, a), \sigma^2 I)$, and the next state from the expert is also $s'_{*,i} \sim \mathcal{N}(\mu(s, a), \sigma^2 I)$, so the difference of the two Gaussians $\Delta := s' - s'_{*,i}$ is also a Gaussian $\Delta \sim \mathcal{N}(0, 2\sigma^2 I)$. Taking F to be the CDF of the standard normal distribution, we can rewrite the following:

$$\begin{aligned} P(|s'[j] - s'_{*,i}[j]| \leq \epsilon) &= 1 - P(|s'[j] - s'_{*,i}[j]| \geq \epsilon) \\ &= 1 - 2P(\Delta[j] \leq -\epsilon) \\ &= 1 - 2F\left(\frac{-\epsilon}{\sqrt{2}\sigma}\right) \\ &= \text{erf}\left(\frac{\epsilon}{2\sigma}\right) \end{aligned}$$

Since all variables are IID, we can thus rewrite the coverage probability as follows:

$$\begin{aligned} P_S(s; N, \epsilon) &= 1 - \prod_{i=1}^N \left(1 - \prod_{j=1}^d P(|s'[j] - s'_{*,i}[j]| \leq \epsilon) \right) \\ &= 1 - (1 - \text{erf}(\frac{\epsilon}{2\sigma})^d)^N \end{aligned}$$

□

We visualize the P_S coverage function on the left side of Fig. 3 under varying amounts of system noise, for different sample sizes N .

A.1 Generalization under System Noise

Definition 2. Given a policy π_A , a data generating policy π_E and a starting state s , define the probability of next state coverage $P_B(s; N) = P(\|s' - c\|_{\infty} \leq \max_{i \in \{1 \dots N\}} \|s'_i - c\|_{\infty})$, where

$s'_i \sim \rho_{\pi_E}^t(\cdot|s)$ are next state samples from the expert starting at s , and $s'_i \sim \rho_{\pi_A}^t(\cdot|s)$ is a sample from π_A starting at s , and $c = \frac{1}{N} \sum_i^N s'_i$ is the sample ‘‘center’’.

Intuitively $P_B(s; N)$ is the probability that given N samples starting at s , the hyper-sphere defined by the samples also contains the sample under the learned policy. The hyper-sphere is centered at the average next state (under expert samples), and the radius fits all the expert data sampled next states (i.e., with radius $\max_{i \in \{1 \dots N\}} \|s'_i - c\|_\infty$). Here the hyper-sphere represents the set of next states that the policy can generalize to. For policies learned with neural networks, this aims to represent the ‘‘interpolation’’ capacity of these models among the training samples.

Theorem A.1. *Given a policy π_A and deterministic demonstrator π_E , assume that for state s , if $\rho_{\pi_E}^{t-1}(s) > 0$, then $\pi_A(a|s) = \mathcal{N}(\pi_E(s), \sigma_\pi^2 I)$. Assume that transitions are normally distributed with fixed and diagonal variance, $\rho(s'|s, a) = \mathcal{N}(\mu(s, a), \sigma^2 I)$, where $\mu(s, a) = s + \alpha a$ are simplified linear dynamics for scalar $\alpha \in \mathbb{R}$. Then the next state coverage probability is $P_B(s; N) = (1 - (\int_0^\infty \frac{2}{\sigma_\pi} f(\frac{x}{\sigma_\pi}) \operatorname{erf}(\frac{x}{\sqrt{2}\sigma_{\pi_E}}))^{Nd})^d$, where d is the dimensionality of the state, f is the PDF of the standard normal, $\sigma_{\pi_E} = \sqrt{(1 + \frac{1}{N})\sigma_s}$, and $\sigma_\pi = \sqrt{\sigma_{\pi_E}^2 + \alpha^2 \sigma_p^2}$.*

Proof. Since samples and dimensions are independent, we can decompose probabilities as follows:

$$\begin{aligned} P_B(s; N) &= P(\|s' - c\|_\infty \leq \max_{i \in \{1 \dots N\}} \|s'_i - c\|_\infty) \\ &= \prod_{j=1}^d P(|s'[j] - c[j]| \leq \max_{i \in \{1 \dots N\}} \|s'_i - c\|_\infty) \\ &= \prod_{j=1}^d (1 - P(|s'[j] - c[j]| > \max_{i \in \{1 \dots N\}} \|s'_i - c\|_\infty)) \\ &= \prod_{j=1}^d (1 - \prod_{i=1}^N P(|s'[j] - c[j]| > \|s'_i - c\|_\infty)) \\ &= \prod_{j=1}^d (1 - \prod_{i=1}^N \prod_{k=1}^d P(|s'[j] - c[j]| > |s'_i[k] - c[k]|)) \end{aligned}$$

Since the dynamics are additive, next state from the policy is $s' \sim \mathcal{N}(s + \pi_E(s), (\sigma^2 + \alpha\sigma_p^2)I)$, while the next state from the expert is $s'_i \sim \mathcal{N}(s + \pi_E(s), \sigma^2 I)$. Thus the center (sample mean) has distribution $c \sim \mathcal{N}(s + \pi_E(s), \frac{1}{N}\sigma^2 I)$. so the difference of the two Gaussians $\Delta_i := s'_i - c$ is also a Gaussian $\Delta_i \sim \mathcal{N}(0, \sigma_{\pi_E}^2 I)$ where $\sigma_{\pi_E}^2 = (1 + \frac{1}{N})\sigma^2$, and similarly for $\Delta := s' - c$, $\Delta \sim \mathcal{N}(0, \sigma_\pi^2 I)$ where $\sigma_\pi^2 = (1 + \frac{1}{N})\sigma^2 + \sigma_p^2$. Taking F to be the CDF of the standard normal distribution and f to be the PDF, by symmetry we can rewrite the following:

$$\begin{aligned} P(|s'[j] - c[j]| \geq |s'_i[k] - c[k]|) &= P(|\Delta[j]| \geq |\Delta_i[k]|) \\ &= 4 \int_0^\infty \frac{1}{\sigma_\pi} f\left(\frac{x}{\sigma_\pi}\right) \int_0^x f\left(\frac{y}{\sigma_{\pi_E}}\right) dy dx \\ &= 4 \int_0^\infty \frac{1}{\sigma_\pi} f\left(\frac{x}{\sigma_\pi}\right) \left(F\left(\frac{x}{\sigma_{\pi_E}}\right) - F(0)\right) dx \\ &= \frac{2}{\sigma_\pi} \int_0^\infty f\left(\frac{x}{\sigma_\pi}\right) \operatorname{erf}\left(\frac{x}{\sqrt{2}\sigma_{\pi_E}}\right) dx \end{aligned}$$

Since all variables are IID, we can thus rewrite the coverage probability as follows

$$P_B(s; N) = \left(1 - \left(\int_0^\infty \frac{2}{\sigma_\pi} f\left(\frac{x}{\sigma_\pi}\right) \operatorname{erf}\left(\frac{x}{\sqrt{2}\sigma_{\pi_E}}\right)\right)^{Nd}\right)^d$$

□

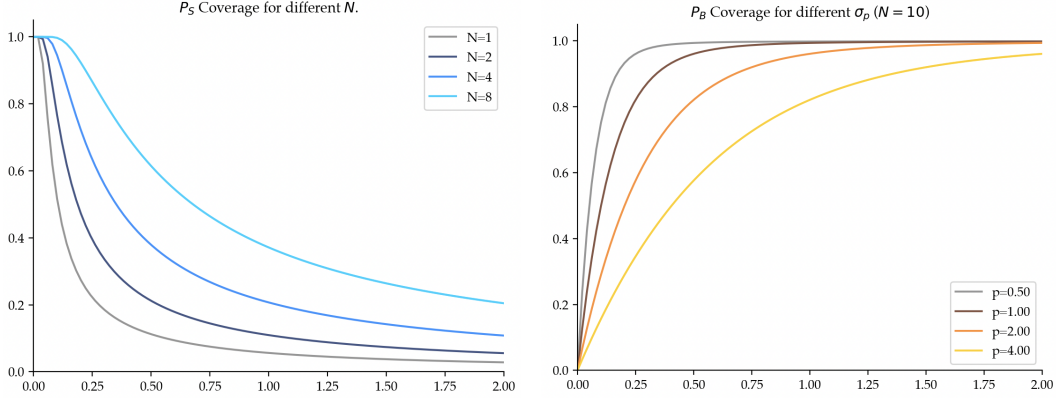


Figure 3: Different coverage functions, where the y-axis denotes coverage probability, and the x-axis is the amount of system noise (standard deviation). **Left:** $P_S(s; N, \epsilon)$ plotted for one-dimensional state under various amounts of data (N). Adding more system noise quickly reduces the likelihood of “coverage” of the test time next state under this conservative definition of coverage, with more robustness as N gets larger. **Right:** $P_B(s; N)$ plotted for one-dimensional state under fixed $N = 10$, but varying the amount of noise in the test time policy. We see that under this more loose coverage model, adding system noise can make coverage likely even under double or triple the noise in the learned policy.

In [Theorem A.1](#), while the probability of next state coverage is not in closed form, we visualize several examples of this function below to gain intuition for how high σ_s can improve the coverage likelihood of the learned policy even under notable σ_p when N is high enough, despite the fact that system noise is present even under the learned policy. We visualize this function on the right side of [Fig. 3](#) under increasing system noise, for various amounts of test time noise σ_p .

B Metrics of Data Quality

Having formalized action divergence and transition diversity in [Sec. 4](#) as two fundamental considerations in a dataset, how can we *measure* these properties in a given dataset?

Action Variance: To measure action consistency, the empirical form of the objective in [Eqn. 7](#) is intractable without access to the underlying expert action distribution π_E . Instead we propose using the empirical variance of the action distribution in the data to approximate the “spread” of the data. In continuous state spaces, we can estimate variance using a coverage distance ϵ to cluster nearby states, and then measuring the per dimension variance across the corresponding actions within said cluster. Defining a cluster to be $C(s, \mathcal{D}) = \{\tilde{s}, \tilde{a}, \tilde{s}' \in \mathcal{D} : \|s - \tilde{s}\| \leq \epsilon\}$, we can compute the variance as:

$$\text{ActionVariance}(\mathcal{D}) = \frac{1}{|D|} \sum_{s, a \in \mathcal{D}} \left(a - \sum_{\tilde{s}, \tilde{a}, \tilde{s}' \in C(s, \mathcal{D})} \tilde{a} \right)^2 \quad (9)$$

The choice in ϵ corresponds to the *generalization* of the learning model to nearby states, similar to the notion of coverage in [Definition 1](#). We use this metric of action consistency in [Sec. 5](#) to study human generated datasets of various quality.

State Similarity: To measure the consistency of states, we approximate the number of “nearby” states using the same clustering process as in the Action Variance metric, and measure the expected cluster size as a fraction of the overall data.

$$\text{StateSimilarity}(\mathcal{D}) = \frac{1}{|D|} \sum_{s, a \in \mathcal{D}} |C(s, \mathcal{D})| \quad (10)$$

While these approximate forms do not encapsulate the full spectrum of possible metrics, we believe these metrics help advance our empirical understanding of data quality for imitation learning. In [section 5.2](#) in the main text, we analyze these metrics of data quality in several environments across different dataset sources.

C Results

The performance results under system noise, policy noise, and both noises are shown with a broader sweep for both *PMObstacle* and *Square* in the tables below.

	$\sigma_s = 0.01$	$\sigma_s = 0.02$	$\sigma_s = 0.03$	$\sigma_s = 0.04$	$\sigma_s = 0.01$	$\sigma_s = 0.02$	$\sigma_s = 0.03$	$\sigma_s = 0.04$
SCRIPTED	100	100	99	96				
$\sigma_s = 0.01$	97.7(1.5)	95.7(0.7)	96.7(1.1)	93.3(0.7)	90.3(7.1)	90.0(8.2)	94.0(2.9)	87.7(3.7)
$\sigma_s = 0.02$	98.7(0.5)	98.0(0.5)	97.7(1.0)	92.7(1.2)	99.7(0.3)	98.0(0.9)	94.3(1.4)	92.3(2.0)
$\sigma_s = 0.03$	98.3(0.7)	98.0(0.8)	99.0(0.5)	95.0(0.9)	99.7(0.3)	98.7(0.5)	97.7(0.5)	95.7(1.1)
$\sigma_s = 0.04$	100.0(0.0)	100.0(0.0)	99.3(0.3)	96.7(0.7)	100.0(0.0)	99.0(0.5)	98.7(0.5)	96.7(1.4)

Table 2: **System Noise:** Success rates (and standard error) for BC in PMObstacle, for 1000 episodes (left) and 10 episodes (right) of data, under system noise. Rows correspond to injecting gaussian system noise (σ_s) into the *dataset* of increasing variance, and columns correspond to injecting noise during *evaluation*. The diagonal in both sub-tables represents evaluating in distribution. **Left:** For large datasets, higher system noise during evaluation tends to decrease the performance of each model (rows left to right), but more system noise during training generally produces the best models (columns top to bottom). **Right:** For small datasets, we observe a similar but exaggerated effect as the left table.

	$\sigma_s = 0.01$	$\sigma_s = 0.02$	$\sigma_s = 0.03$	$\sigma_s = 0.04$	$\sigma_s = 0.01$	$\sigma_s = 0.02$	$\sigma_s = 0.03$	$\sigma_s = 0.04$
SCRIPTED	100	100	99	96				
$\sigma_p = 0.01$	94.0(1.7)	94.0(2.4)	94.7(1.8)	91.3(1.4)	78.0(8.6)	78.7(6.7)	81.3(5.0)	81.3(5.8)
$\sigma_p = 0.02$	87.7(2.0)	92.3(2.0)	90.7(2.0)	91.3(2.2)	88.0(9.4)	78.7(4.4)	80.7(3.1)	80.3(3.2)
$\sigma_p = 0.03$	97.0(0.9)	99.0(0.5)	97.0(0.0)	95.0(0.8)	88.7(3.2)	82.7(5.4)	88.7(5.2)	85.7(4.4)
$\sigma_p = 0.04$	86.7(4.3)	91.0(2.4)	93.3(1.4)	92.7(1.5)	88.3(6.5)	88.0(4.5)	86.0(5.9)	82.3(2.0)

Table 3: **Policy Noise:** Success rates (and standard error) for BC in PMObstacle, for 1000 episodes (left) and 10 episodes (right) of data, under learned policy noise. Rows correspond to injecting gaussian policy noise (σ_p) into the *expert* of increasing variance, and columns correspond to injecting system noise during *evaluation*. **Left:** For large datasets, unlike system noise in Table 2, more policy noise during training often produces the worst models (columns top to bottom). **Right:** For small datasets, adding policy noise produces large variance in performance across runs. Importantly, the datasets in each row have the same observed state diversity as the corresponding row in Table 2, but performance is almost universally lower in both sub-tables here, supporting the idea that state diversity is a coarse metric for success.

	$\sigma_s = 0.01$	$\sigma_s = 0.02$	$\sigma_s = 0.03$	$\sigma_s = 0.04$	$\sigma_s = 0.01$	$\sigma_s = 0.02$	$\sigma_s = 0.03$	$\sigma_s = 0.04$
SCRIPTED	100	100	99	96				
$\sigma_p = 0.01$	96.3(2.2)	99.3(0.5)	97.7(0.3)	93.3(1.0)	99.7(0.3)	98.0(1.2)	96.7(0.5)	96.3(1.4)
$\sigma_p = 0.02$	98.0(0.5)	98.3(0.5)	97.7(0.7)	94.7(1.0)	99.3(0.5)	98.7(1.1)	96.0(2.2)	94.7(1.7)
$\sigma_p = 0.03$	98.0(0.8)	96.7(1.0)	98.3(1.0)	96.3(0.7)	95.0(2.1)	97.7(0.5)	97.7(0.5)	93.3(2.2)
$\sigma_p = 0.04$	98.7(0.5)	99.0(0.5)	97.3(0.3)	95.0(0.8)	100.0(0.0)	99.7(0.3)	99.0(0.8)	93.7(3.1)

Table 4: **System Noise + Policy Noise:** Success rates (and standard error) for BC in PMObstacle, for 1000 episodes (left) and 10 episodes (right) of data, under learned policy noise for a fixed amount of system noise ($\sigma_p = 0.03$). Here we see how system noise improves the robustness of the model to added policy noise.

	$\sigma_s = 0.05$	$\sigma_s = 0.1$	$\sigma_s = 0.2$	$\sigma_s = 0.3$	$\sigma_s = 0.4$
$\sigma_s = 0.05$	55.7(5.3)	50.0(5.4)	27.0(3.9)	12.0(2.4)	7.3(2.2)
$\sigma_s = 0.1$	69.7(5.5)	69.0(3.7)	57.3(6.0)	50.3(6.0)	22.7(3.5)
$\sigma_s = 0.2$	67.7(9.6)	68.7(12.6)	82.0(3.4)	74.3(2.7)	50.3(1.7)
$\sigma_s = 0.3$	47.0(4.9)	53.3(5.9)	54.3(3.0)	50.7(4.3)	38.7(7.3)
$\sigma_s = 0.4$	31.3(5.0)	37.7(8.2)	48.3(9.7)	49.0(8.7)	44.0(5.3)

Table 5: **System Noise, 200ep**: Success rates for BC in Square, for 200 episodes of data, under system noise. Rows correspond to injecting gaussian system noise (σ_s) into the *dataset* of increasing variance, and columns correspond to injecting noise during *evaluation*. The diagonal in both sub-tables represents evaluating in distribution. In both sub-tables we see how policies with low data coverage (low system noise) generalize the worst to increasing noise at test time. More system noise during training generally produces the best models (columns top to bottom).

	$\sigma_s = 0.05$	$\sigma_s = 0.1$	$\sigma_s = 0.2$	$\sigma_s = 0.3$	$\sigma_s = 0.4$
$\sigma_s = 0.05$	40.0(1.2)	33.7(3.1)	16.7(1.4)	4.3(1.0)	2.0(0.5)
$\sigma_s = 0.1$	42.3(4.0)	39.7(3.8)	31.3(3.7)	19.7(3.1)	10.0(1.6)
$\sigma_s = 0.2$	70.0(7.0)	73.7(5.4)	69.7(0.7)	55.3(1.2)	27.0(2.2)
$\sigma_s = 0.3$	57.3(3.1)	58.7(3.1)	64.7(1.4)	60.7(0.3)	44.7(2.2)
$\sigma_s = 0.4$	30.0(7.0)	33.7(6.4)	39.7(5.7)	39.7(6.5)	36.7(6.9)

Table 6: **System Noise, 50ep**: Success rates for BC in Square, for 50 episodes of data, under system noise. Rows correspond to injecting gaussian system noise (σ_s) into the *dataset* of increasing variance, and columns correspond to injecting noise during *evaluation*. The diagonal in both sub-tables represents evaluating in distribution. In both sub-tables we see how policies with low data coverage (low system noise) generalize the worst to increasing noise at test time. More system noise during training generally produces the best models (columns top to bottom).

	$\sigma_p = 0.005$	$\sigma_p = 0.01$	$\sigma_p = 0.02$	$\sigma_p = 0.05$	$\sigma_p = 0.1$
$\sigma_p = 0.005$	69.0(3.7)	59.0(3.7)	34.0(1.7)	20.7(2.4)	7.0(1.6)
$\sigma_p = 0.01$	80.7(3.7)	78.0(4.2)	57.7(2.4)	38.0(1.7)	23.0(2.2)
$\sigma_p = 0.02$	62.3(7.8)	71.7(6.1)	73.0(3.9)	65.3(2.8)	43.3(3.6)

Table 7: **Policy Noise, 200ep**: Success rates for BC in Square, for 200 episodes of data, under learned policy noise. Rows correspond to injecting gaussian policy noise (σ_p) into the *dataset* of increasing variance, and columns correspond to injecting noise during *evaluation*. In the high data regime, we see that more policy noise tends to improve performance (columns top to bottom), since the noise is unbiased so with enough samples from the scripted policy, the model will recover an unbiased policy.

	$\sigma_p = 0.005$	$\sigma_p = 0.01$	$\sigma_p = 0.02$	$\sigma_p = 0.05$	$\sigma_p = 0.1$
$\sigma_p = 0.005$	32.7(3.8)	30.3(3.2)	18.0(3.6)	7.0(0.8)	5.7(1.2)
$\sigma_p = 0.01$	61.3(4.3)	59.0(6.7)	48.3(3.7)	29.7(1.7)	19.3(1.4)
$\sigma_p = 0.02$	57.7(3.2)	58.3(3.1)	49.3(0.5)	41.3(0.5)	28.3(2.4)

Table 8: **Policy Noise, 50ep**: Success rates for BC in Square, for 50 episodes of data, under learned policy noise. Rows correspond to injecting gaussian policy noise (σ_p) into the *dataset* of increasing variance, and columns correspond to injecting noise during *evaluation*. As the amount of data is reduced, there is a significant drop in performance for added policy noise in the dataset, along with higher performance variation compared to 200eps, since the policy can no longer recover an unbiased policy.